DOI: 10.1021/ma101194y

Macromolecules
ARTICLE

On the Favorable Interaction of Metal Centered Radicals with Hydroperoxides for an Enhancement of the Photopolymerization Efficiency Under Air

Jacques Lalevée,*,† Mohamad-Ali Tehfe,† Didier Gigmes,‡ and Jean Pierre Fouassier†

†*Department of Photochemistry, CNRS, University of Haute Alsace, Ecole Nationale Supérieure de Chimie de Mulhouse, 3 rue Alfred Werner, 68093 Mulhouse Cedex, France, and* ‡*UMR 6264 Laboratoire Chimie Provence, Université de Provence, Avenue Escadrille Normandie-Niemen, Case 542, Marseille 13397, Cedex 20, France*

Received May 28, 2010; Revised Manuscript Received June 16, 2010

ABSTRACT: Four metal-based photoinitiating systems (benzene−tricarbonylchromium(0), $ArCr(CO)_3$, cyclopentadienylmolybdenum tricarbonyl dimer, $Cp_2Mo_2(CO)_6$, diiron nonacarbonyl, $Fe_2(CO)_9$, and bis-(cyclopentadienylruthenium dicarbonyl), $Cp_2Ru_2(CO)_4$) are investigated by laser flash photolysis (LFP) and ESR−spin trapping (ESR−ST) experiments and checked as photoinitiators for both free radical promoted cationic photopolymerization (FRPCP) and free radical photopolymerization (FRP). New combinations with silanes instead of alkyl halides improve both the polymerization rates and the final conversions upon irradiation with UV/visible or visible light and laser diodes (405, 457, 473, and 532 nm) under air. The enhancement of the photopolymerization reaction under air in the presence of the selected compounds is ascribed to the reuse of the inherently present hydroperoxides through a set of reactions leading to additional initiating species. These systems are particularly attractive for FRPCP with excellent polymerization rates and final conversions.

Introduction

The development of new photoinitiating systems for free radical promoted cationic photopolymerization FRPCP and/or free radical photopolymerization FRP processes still remains a matter of concerns.[1,2] Indeed, photoinitiated processes are characterized by important advantages compared to thermal reactions, i.e., (i) the polymerization reaction can be spatially controlled and can easily be turned on or off at will, and (ii) most photopolymerization processes operate without solvents and thus meet the actual demands of green chemistry.[1,2] FRPCP is an elegant method where radicals ($R^\bullet$) are first generated from suitable PIs and then oxidized by a diaryliodonium salt, the resulting cations (R^+) being the main cationic polymerization initiating structures.[3] The design of sources of efficient radicals has been the subject of huge research efforts. They are mostly generated from organic compounds in type **I** cleavable photoinitiators PI or type **II** photoinitiating systems based on a hydrogen transfer reaction between a photoinitiator PI and a co-initiator.[1,2]

The commonly encountered drawback of FRPCP and FRP is the well-known oxygen inhibition due to the formation of peroxyls $RO_2^\bullet$ (1);[4] $RO_2^\bullet$s do not add to a monomer double bond in FRP and can be hardly oxidized in FRPCP thereby leading to a decrease of the polymerization efficiency for both processes.[1,2,5] In low viscosity samples, the situation is worse as the reoxygenation of the formulation remains efficient during the whole photopolymerization process leading to strongly reduced monomer conversions. In recent papers, we have outlined the specific, versatile and valuable role of the silyl radicals which allows to overcome this problem for FRPCP and FRP and to propose a lot of type I and type II systems being able to efficiently work (with high polymerization rates and final conversions) even in low viscosity monomers, under air, upon UV or visible light (Hg lamp, Xe lamp, laser diodes, sunlight) and at low light intensity.[5−8] The set of reactions 2−7 recalls that the key reactions[6a,8] e.g. when using silanes $R_1R_2R_3Si-H$ in Type I or Type II PI, are (i) the formation of silyls 2 and 3, (ii) the conversion of the peroxyls into new initiating silyl radicals through a hydrogen abstraction reaction 4a, (iii) the conversion of the peroxyls into hydroperoxides by hydrogen abstraction processes from polymer chains (P−H) 4b, (iv) the high efficient peroxylation process that consumes oxygen 5 and then leads to a regeneration of the silyl radicals 6 and 7. When using more exotic co-initiators based on a multivalent atom containing structure such as various metal amines M−R′ (M = Si, Ti, Zr and P), reaction was also turned to a bimolecular homolytic substitution (S_H2) reaction 8, the formed peroxide R-OOM being able to be further decomposed.[8]

$$R^\bullet + O_2 \rightarrow RO_2^\bullet \quad (1)$$

$$^*PI + R_1R_2R_3Si-H \rightarrow PIH^\bullet + R_1R_2R_3Si^\bullet \quad (2a)$$

$$^*PI \rightarrow R'^\bullet \quad \text{and} \quad R'^\bullet + R_1R_2R_3Si-H \rightarrow R_1R_2R_3Si^\bullet \quad (2b)$$

$$R^\bullet + R_1R_2R_3Si-H \rightarrow RH + R_1R_2R_3Si^\bullet \quad (3)$$

$$RO_2^\bullet + R_1R_2R_3Si-H \rightarrow ROOH + R_1R_2R_3Si^\bullet \quad (4a)$$

$$RO_2^\bullet + P-H \rightarrow ROOH + P^\bullet \quad (4b)$$

$$R_1R_2R_3Si^\bullet + O_2 + R_1R_2R_3SiOO^\bullet \quad (5)$$

$$R_1R_2R_3SiOO^\bullet + R_1R_2R_3Si-H \rightarrow R_1R_2R_3SiOOH + R_1R_2R_3Si^\bullet \quad (6)$$

*Corresponding author. E-mail: j.lalevee@uha.fr.

 Published on Web 07/21/2010

Scheme 1

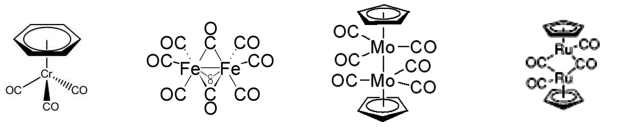

$$R_1R_2R_3SiOO^{\bullet} \rightarrow R_1Si^{\bullet}(OR_2)(OR_3) \quad (7)$$

$$R\text{-}O_2^{\bullet} + M - R'^{\bullet} \rightarrow R - OOM + R'^{\bullet} \quad (8)$$

The only way to still improve the performance of a PI/silane photoinitiating system working under air consists in acting on the hydroperoxides generated in 4 and 6. For FRPCP, silyl radicals generated in 2, 3, 4a, 6, and 7 can be oxidized by iodonium salts leading to silylium cations which can initiate the ring-opening polymerization of epoxy monomers.[5b,c] The basic idea in the present paper is therefore to propose a new concept based on the decomposition of the hydroperoxides 9 which should allow the generation of additional initiating radicals: an alkoxyl and a hydroxyl radical 9 or/and a new silyl radical 10.

$$R - OOH \rightarrow RO^{\bullet} + OH^{\bullet} \quad (9)$$

$$RO^{\bullet} + R_1R_2R_3Si - H \rightarrow ROH + R_1R_2R_3Si^{\bullet} \quad (10)$$

The main problem is however to design a photoinitiating system that can induce such reactions as seen in eqs 9 and 10 in situ. It is known in the literature that the $CpW^{\bullet}(CO)_3$ radical is able to decompose hydroperoxides with the formation of alkoxyl radicals.[9] We therefore decided to pay attention to the metal based photoinitiator family (**MB-PIs**) combined with silane compounds (the general interest of **MB-PIs** in FRP has already been highlighted in different works).[10−12] The proposed systems are based on four selected compounds **M-Sub** (where M = molybdenum, chromium, iron and ruthenium and **Sub** stands for the substituents) and various **M-Sub**/silane (tris(trimethylsilyl)silane, TTMSS) combinations (Scheme 1). The ability of these systems to initiate the FRPCP of an epoxide (upon addition of an iodonium salt) as well as the FRP will be checked under air. The overall initiation mechanism and the decomposition of the hydroperoxides will be investigated by laser flash photolysis (LFP) and ESR−spin trapping (ESR−ST) experiments.

Experimental Part

i. Compounds. The investigated compounds are shown in Scheme 1. Benzene−tricarbonylchromium(0) ($ArCr(CO)_3$), cyclopentadienylmolybdenum tricarbonyl dimer ($Cp_2Mo_2(CO)_6$), diiron nonacarbonyl ($Fe_2(CO)_9$), bis(cyclopentadienylruthenium dicarbonyl) ($Cp_2Ru_2(CO)_4$), diphenyl iodonium hexafluorophosphate (Ph_2I^+), and tris(trimethylsilyl)silane (TTMSS) were obtained from Aldrich and used with the best purity available. (3,4-Epoxycyclohexane)methyl 3,4-epoxycyclohexylcarboxylate (EPOX, UVACURE 1500) and TMPTA (trimethylolpropane triacrylate) were gifts of Cytec.

ii. Free Radical Promoted Cationic Polymerization (FRPCP). In FRPCP experiments, the different photoinitiating systems **M-Sub**/TTMSS/Ph_2I^+ are based on **M-Sub** (1% w/w) and 1% w/w in diphenyliodonium hexafluorophosphate Ph_2I^+ (except as otherwise noted). TTMSS was used as an additive (3% w/w). For $Cp_2Ru_2(CO)_4$/TTMSS/Ph_2I^+, a very slow degradation of the formulation was noted. This does not prevent, however, the study of the photoinitiating ability on fresh samples. The EPOX films (25 μm thick) deposited were irradiated on a BaF_2 pellet. The evolution of the epoxy group content at about 790 cm^{-1} is continuously followed by real time FTIR spectroscopy (Nexus 870, Nicolet) as reported in refs 5 and 7

iii. Free Radical Polymerization (FRP). For film polymerization experiments, TMPTA was used as a low viscosity monomer (∼100 cP). The **M-sub**s were dissolved in this medium (1% w/w); TTMSS was used as an additive (3% w/w). The films (20 μm thick) deposited on a BaF_2 pellet were irradiated with various light sources (see hereafter). The evolution of both the double bond and Si−H contents was continuously followed by real time FTIR spectroscopy (Nexus 870, Nicolet) at about 1630 and 2050 cm^{-1}, respectively.[5,6] Because of the quite slow polymerization process and the low viscosity of the samples, the change of the sample thickness throughout the photopolymerization reaction induces an error larger than previously seen in refs 5 and 6 on the final conversion: it can be evaluated up to 10%.

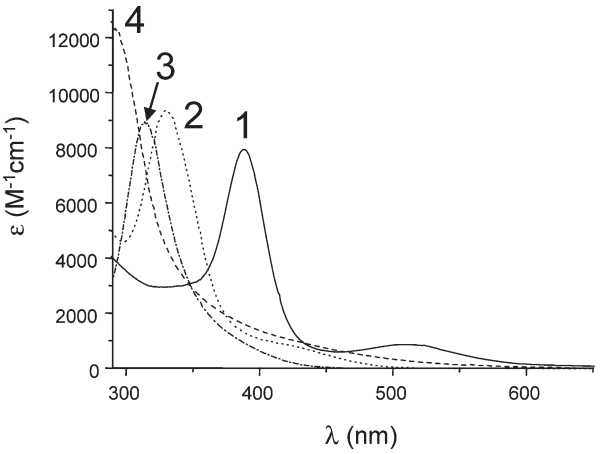

Figure 1. UV−visible absorption spectra: (1) $Cp_2Mo_2CO_6$; (2) $Cp_2Ru_2CO_4$; (3) $ArCrCO_3$ in *tert*-butylbenzene; (4) Fe_2CO_9 in acetonitrile.

iv. Irradiation Sources. Several light sources have been used: Xe−Hg lamp (Hamamatsu, L8252, 150 W; polychromatic UV−visible light; $I \sim 22$ mW/cm^2 in the 300−400 nm range), Xe lamp (filtered light at $\lambda > 390$ nm; Hamamatsu, L8253, 150 W; $I \sim 60$ mW/cm^2 in the 390−800 nm range), monochromatic lights delivered by laser diodes at 405 nm (cube−continuum; $I_0 \sim 12$ mW cm^{-2}), 457 nm (MBL-F-457- BFIOPTILAS; $I_0 \sim 100$ mW cm^{-2}), 473 nm (MBL-III-473- BFIOPTILAS; $I_0 \sim 100$ mW cm^{-2}), and 532 nm (MGL-III-532- BFIOPTILAS; $I_0 \sim 100$ mW cm^{-2}).

v. ESR Spin Trapping (ESR−ST) Experiments. ESR−ST experiments were carried out using a X-Band spectrometer (MS 200 Magnettech). The radicals were produced at RT under a xenon lamp exposure ($\lambda > 300$ nm) and trapped by phenyl-*N*-*tert*-butylnitrone (PBN) according to a procedure described in detail in refs 13 and 14

vi. Laser Flash Photolysis (LFP). The nanosecond laser flash photolysis LFP experiments were carried out with a Q-switched nanosecond Nd/YAG laser at $\lambda_{exc} = 355$ nm (9 ns pulses; energy reduced down to 10 mJ; Powerlite 9010 Continuum), the analyzing system consisting in a pulsed xenon lamp, a monochromator, a fast photomultiplier, and a transient digitizer.[15]

Results and Discussion

1. Absorption Properties of M-Subs. The absorption properties of the investigated compounds are depicted in Figure 1. The absorption can be easily tuned through an appropriate selection of the **M-Sub**s, i.e., $ArCr(CO)_3$, $Cp_2Mo_2(CO)_6$, $Fe_2(CO)_9$, and $Cp_2Ru_2(CO)_4$, present maximum absorptions at 315, 388, ∼290, and 330 nm, respectively, spread over the visible range and exhibit high molar absorption coefficients at 405 nm (∼540, 4800, 1300, and 1000 M^{-1} cm^{-1} for $ArCr(CO)_3$, $Cp_2Mo_2(CO)_6$, $Fe_2(CO)_9$, and $Cp_2Ru_2(CO)_4$, respectively) that are significantly higher than those reported for classical organic photoinitiators.[2c] Interestingly, significant absorptions are also noted at classical laser irradiation wavelengths (e.g., 750 M^{-1} cm^{-1} at 532 nm for $Cp_2Mo_2(CO)_6$).

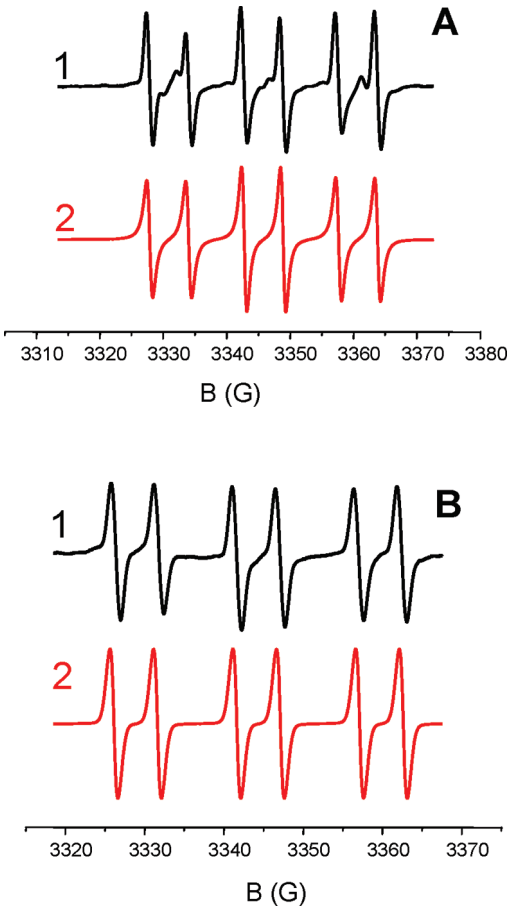

Figure 2. ESR spin trapping experimental (1) and simulated (2) spectrum obtained upon irradiation of (A) $Fe_2(CO)_9$/TTMSS and (B) $ArCr(CO)_3$/TTMSS. Xenon lamp exposure. PBN 0.05 M. See text.

2. Photochemistry of M-Subs. *2.1. Silyl Radical Generation As Evidenced by ESR−ST.* When the four **M-Subs** are irradiated in the presence of PBN, no PBN adduct is observed. Upon the addition of TTMSS, the tris(trimethylsilyl)silyl radical is easily detected (e.g., Figure 2); i.e., the hyperfine coupling constants of the PBN adduct (a_N = 15.3; a_H = 5.4 G) are in agreement with the already known values.[5a,16] The new proposed **M-Sub**/TTMSS systems should be very attractive for both FRP and FRPCP as the silyl radical formed in 11 efficiently adds to acrylates (2.2×10^7 M^{-1} s^{-1} to methyl acrylate) and is easily oxidized by iodonium salts (2.6×10^6 M^{-1} s^{-1}).[5b,c,17,18]

$$\textbf{M-Sub} + R_1R_2R_3Si{-}H \rightarrow \rightarrow R_1R_2R_3Si^{\bullet} \quad (h\nu) \qquad (11)$$

2.2. Excited State Processes: Laser Flash Photolysis

2.2.1. $Cp_2Mo_2(CO)_6$ and $Cp_2Ru_2(CO)_4$: Metal−Metal Bond Cleavage. In agreement with previous studies,[19,20] the laser excitation of $Cp_2Mo_2(CO)_6$ and $Cp_2Ru_2(CO)_4$ at 355 nm leads to a bleaching (Figure 3) observed within the laser pulse (the dissociation rate constants k_{diss} are $> 10^8$ s^{-1}). The recovery of the starting molecule is associated with the recombination of the radicals formed in the metal−metal bond cleavage process ($CpMo^{\bullet}(CO)_3$ or $CpRu^{\bullet}(CO)_2$).[20] The radicals cannot be directly observed but their reactivity is easily probed: in the absence of any quencher, a quantitative recovery of the absorbance is found (Figure 3A); in the presence of a quencher, the extent of the **M-Sub** recovery is strongly reduced and the rate at which the metal radical disappears is accelerated. The variation of the pseudo

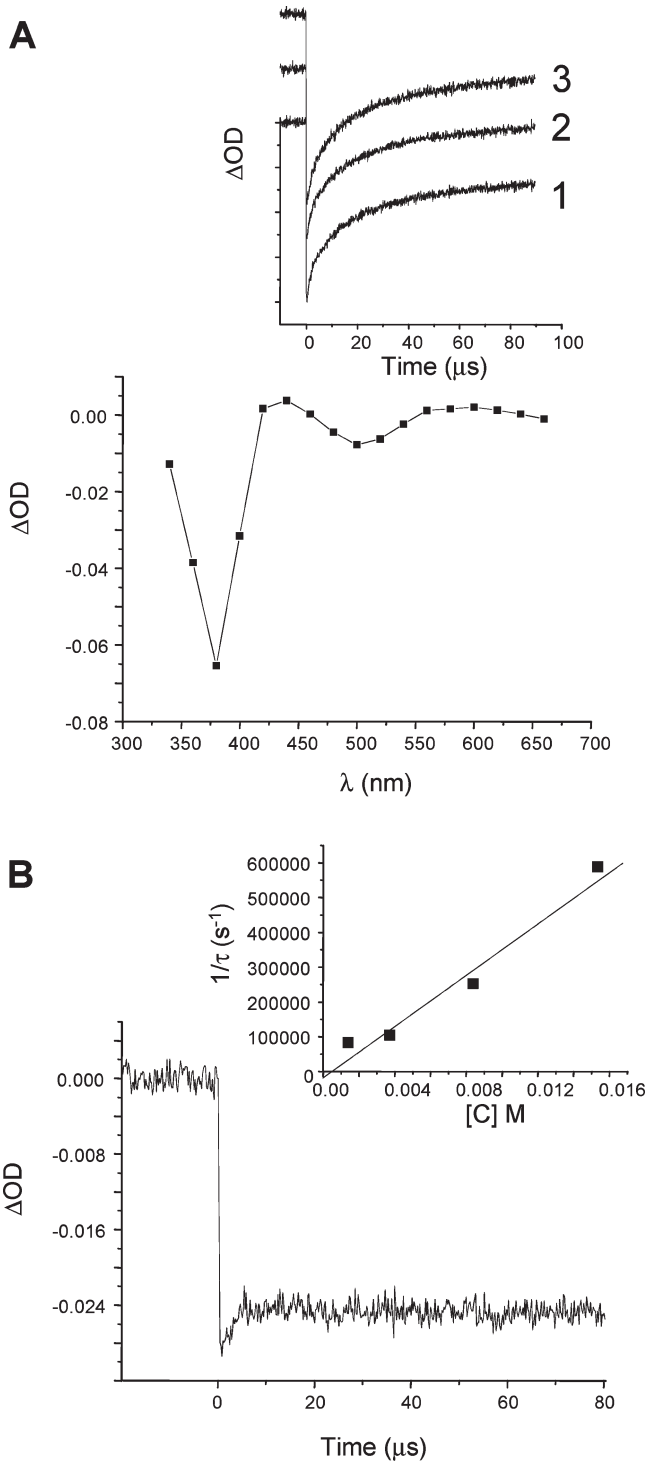

Figure 3. (A) Transient absorption spectra obtained at t = 1 μs after the Nd/YAG laser excitation of $Cp_2Mo_2(CO)_6$. Inset: kinetics at 360 nm for different TTMSS concentrations—(1) 0 M; (2): 0.075 M; (3): 0.15 M in acetonitrile. (B) kinetics at 360 nm for [3-chloroperbenzoic acid] = 0.015 M in acetonitrile. Inset: Stern−Volmer plot for the $CpMo^{\bullet}(CO)_3$/3-chloroperbenzoic acid interaction.

first order rate constants with the quencher concentration (Figure 3B) allows to determine the radical/quencher interaction bimolecular rate constants gathered in Table 1. These radicals do not exhibit a high addition rate constant to MA or EPOX but efficiently reacts with oxygen (rate constants close to the diffusion limit $\sim 3 \times 10^9$ M^{-1} s^{-1}) and present a relatively low interaction with TTMSS (hydrogen abstraction rate constants $< 2 \times 10^5$ M^{-1} s^{-1} as in other metal

Table 1. Reactivity of the Metal-Centered Radicals toward O_2, Methylacrylate (MA), Tris(trimethylsilyl)silane (TTMSS), Diphenyl Iodonium Hexafluorophosphate (Ph_2I^+), EPOX, and Cumene Hydroperoxide (CumOOH): Interaction Rate Constants k (M^{-1} s^{-1}) in *tert*-butylbenzene

	O_2	MA	TTMSS	Ph_2I^+	EPOX	CumOOH
$CpMo^{\bullet}(CO)_3$	3.2×10^9	$< 10^5$ [a]	$< 2 \times 10^5$ [a]	$< 1.0 \times 10^7$ [a]	$< 5 \times 10^5$	2.2×10^6; 1.5×10^6 [a] (3.7×10^7 [b])
$CpRu^{\bullet}(CO)_2$		$< 10^5$	$< 2 \times 10^5$	$< 5.0 \times 10^6$ [a]	$< 5 \times 10^5$	c

[a] In acetonitrile. [b] For 3-chloroperbenzoic acid. [c] The degradation of $Cp_2Ru_2(CO)_4$ solution with addition of CumOOH prevents this experiment.

centered radical/silane interactions[11h,16]). The oxidation of these investigated metal radicals by Ph_2I^+ is also quite hard (Table 1).

$$Cp_2Mo_2(CO)_6 \rightarrow CpMo^{\bullet}(CO)_3 + CpMo^{\bullet}(CO)_3 \quad (12a)$$

$$Cp_2Ru_2(CO)_4 \rightarrow CpRu^{\bullet}(CO)_2 + CpRu^{\bullet}(CO)_2 \quad (12b)$$

$$CpMo^{\bullet}(CO)_3 + R_1R_2R_3Si-H \rightarrow CpMo(CO)_3H + R_1R_2R_3Si^{\bullet} \quad (13a)$$

$$CpRu^{\bullet}(CO)_2 + R_1R_2R_3Si-H \rightarrow CpRu(CO)_2H + R_1R_2R_3Si^{\bullet} \quad (13b)$$

2.2.2. $ArCr(CO)_3$ and $Fe_2(CO)_9$: the CO loss. Upon laser excitation, a bleaching of $ArCr(CO)_3$ is observed at 330 nm and weak absorptions corresponding to $ArCr(CO)_2$ are noted at about 280 and 400 nm as already described.[21] The $ArCr(CO)_2$/TTMSS interaction is low (rate constant $< 3 \times 10^5$ M^{-1} s^{-1}) but a tris(trimethylsilyl)silyl radical is formed (see ESR−ST above): this presumably occurs through a quite complex set of reactions (as proposed in $ArCr(CO)_3/CCl_4$[10,11a−11g,12,21]) involving a CO loss which is also observed here (decrease of the ν(CO) bands at about 1950 cm^{-1} under light irradiation; Supporting Information − Figure 1).

$$ArCr(CO)_3 \rightarrow ArCr(CO)_2 + CO$$

$$ArCr(CO)_2 + R_1R_2R_3Si-H \rightarrow R_1R_2R_3Si^{\bullet} + \text{products} \quad (14)$$

A similar CO lost is also expected in $Fe_2(CO)_9$ as the low temperature UV/vis photolysis of this compound yields the $Fe_2(CO)_8$ unsaturated complex producing both CO-bridged and unbridged isomers:[22] On the basis of previous works,[22] the weak and noisy transient observed at $\lambda < 350$ nm by LFP is tentatively ascribed to $Fe_2(CO)_8$. This transient is not dramatically affected by TTMSS ($k < 10^5$ M^{-1} s^{-1}) but the tris(trimethylsilyl)silyl radical is clearly detected in ESR−ST, still evidencing here a complex and unclear set of reactions as shown in eq 15.

$$Fe_2(CO)_9 \rightarrow Fe_2(CO)_8 + CO$$

$$Fe_2(CO)_8 + R_1R_2R_3Si-H \rightarrow R_1R_2R_3Si^{\bullet} + \text{products} \quad (15)$$

*2.2.3. Decomposition of the Hydroperoxides in the Presence of **M-Sub**.* Interestingly, the metal radicals (for **M** = Mo and Ru) or the generated intermediates (for **M** = Fe and Cr) are able to decompose the hydroperoxides e.g. 16 where the interaction rate constant k of $CpMo^{\bullet}(CO)_3$ with cumene hydroperoxide (CumOOH) is about 2×10^6 M^{-1} s^{-1} (Table 1). The solvent is not involved in the process as similar rate constants are found in acetonitrile and *tert*-butylbenzene. $CpMo^{\bullet}(CO)_3$ is also able to decompose a peracid (e.g., $k = 3.7 \times 10^7$ M^{-1} s^{-1} for 3-chloroperbenzoic acid). The reaction of these metal radicals with di-*tert*-butylperoxide,

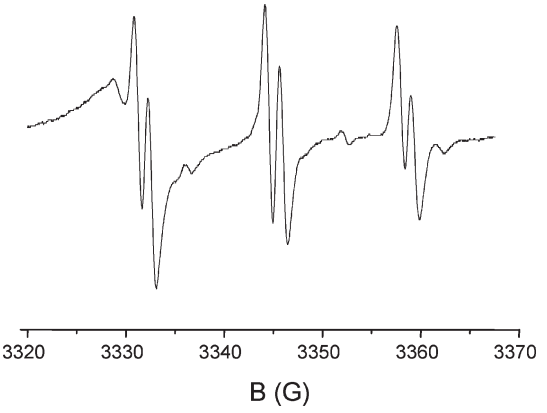

Figure 4. ESR spin trapping spectrum obtained upon irradiation of $Cp_2Mo_2(CO)_6$/CumOOH in *tert*-butylbenzene. Xenon lamp exposure. PBN 0.05 M. The PBN adduct is characterized by $a_N = 13.5$; $a_H = 1.5$ G.

occurs with a lower rate constant ($k < 5 \times 10^5$ M^{-1} s^{-1}).

$$CpMo^{\bullet}(CO)_3 + CumOOH \rightarrow CpMoOH(CO)_3 + CumO^{\bullet} \quad (16)$$

This reaction is also supported by ESR−ST (Figure 4) as the irradiation of a $Cp_2Mo_2(CO)_6$/CumOOH solution leads to the $CumO^{\bullet}$ ($Ph-C(CH_3)_2O^{\bullet}$) alkoxyl radical (PBN adduct: $a_N = 13.5$; $a_H = 1.5$ G in agreement with literature data[13]). Another quite weak signal is ascribed to the methyl radical ($a_N = 14.5$; $a_H = 3.3$ G) generated through the known and previously detected fragmentation of $CumO^{\bullet}$ ($CumO^{\bullet} \rightarrow Ph-C(=O)CH_3 + CH_3^{\bullet}$).[14b] Using $Cp_2Mo_2(CO)_6$ and $Cp_2Ru_2(CO)_4$, the driving factor of the CumOOH decomposition is the formation of strong metal−oxygen bonds leading to highly exothermic reactions i.e. the reaction exothermicities are 73 and 79 kJ/mol for $CpMo^{\bullet}(CO)_3$ and $CpRu^{\bullet}(CO)_2$ respectively (calculated at UB3LYP/LANL2DZ level with the Gaussian suite of programs[23]). In $ArCr(CO)_3$, the generated $ArCr(CO)_2$ species is also quenched by CumOOH ($k = 1.1 \times 10^6$ M^{-1} s^{-1}). This reaction also clearly leads to $CumO^{\bullet}$ as supported by ESR−ST. Because of the too weak signals and the low solubility of $Fe_2(CO)_9$ in *tert*-butylbenzene, no measurement can be done on the $Fe_2(CO)_8$/CumOOH interaction.

3. FRP in Laminate. The expected role of the hydroperoxides is demonstrated (e.g., using a 473 nm diode laser exposure) when comparing the relative efficiency of the **M-Sub**/CumOOH, **M-Sub**/TTMSS and **M-Sub**/TTMSS/CumOOH systems (Figure 5). CumOOH improves the polymerization efficiency and the **M-Sub**/TTMSS/CumOOH system appears as more efficient than the **M-Sub**/alkyl halide usually proposed e.g. in arene chromium complex.[10,11a−11g,12] The inhibition time is reduced and the consumption of the silanes Si−H is almost complete. Moreover, **M-Sub**/CumOOH can also behave as a Type II PI with a polymerization initiating ability quite similar to **M-Sub**/alkyl halide.

4. FRP under Air upon Lamp and Laser Diode Exposure. Using **M-Sub**s alone does not lead to any photopolymerization of TMPTA under air (excepted $ArCr(CO)_3$ (conversion

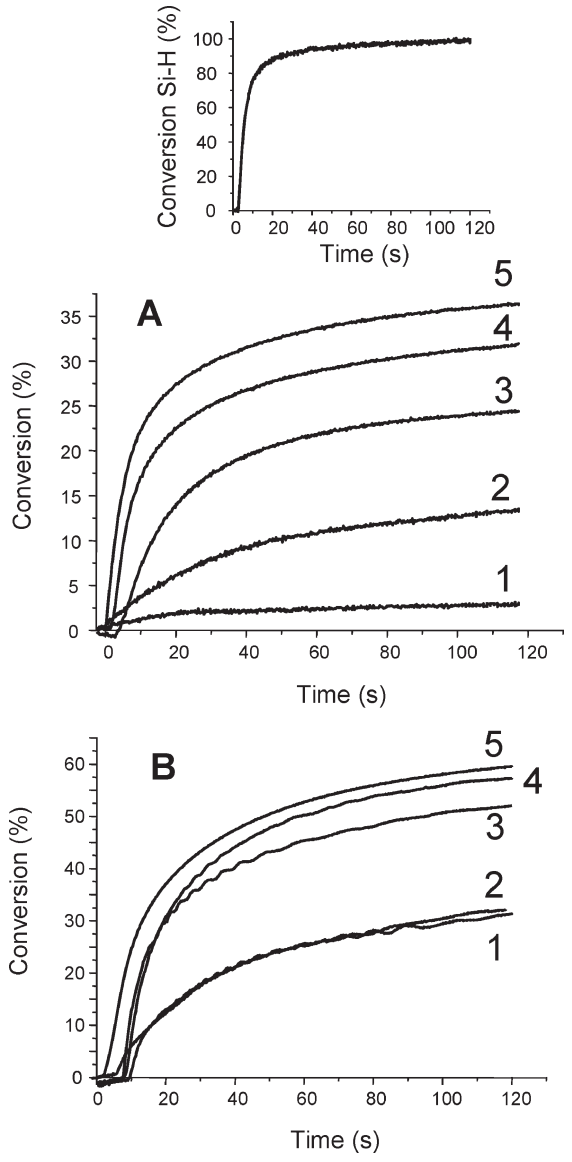

Figure 5. (A) Photopolymerization profiles of TMPTA in laminated conditions upon a diode laser irradiation (473 nm) in the presence of (1) $Cp_2Mo_2(CO)_6$ (1% w/w), (2) $Cp_2Mo_2(CO)_6$/TTMSS (1%/3% w/w), (3) $Cp_2Mo_2(CO)_6$/CumOOH (1%/3% w/w), (4) $Cp_2Mo_2(CO)_6$/CCl_4 (1%/3% w/w), and (5) $Cp_2Mo_2(CO)_6$/CumOOH/TTMSS (1%/3%/3% w/w). Inset: the Si−H conversion for point 5. (B) Photopolymerization profiles of TMPTA in laminated conditions upon a Xe−Hg lamp irradiation ($\lambda > 310$ nm) in the presence of (1) $ArCr(CO)_3$ (1% w/w), (2) $ArCr(CO)_3$/TTMSS (1%/3% w/w), (3) $ArCr(CO)_3$/CCl_4 (1%/3% w/w), (4) $ArCr(CO)_3$/CumOOH (1%/3% w/w), and (5) $ArCr(CO)_3$/CumOOH/TTMSS (1%/3%/3% w/w).

of about 5% at $t = 120$ s upon a Hg−Xe lamp irradiation; see Figure 6). The addition of CCl_4 does not drastically improve the polymerization i.e. nothing is observed in the presence of the $Cp_2Mo_2(CO)_6$ [$Fe_2(CO)_9$, $Cp_2Ru_2(CO)_4$]/CCl_4 systems and only a modest increase of the final conversion (i.e., 10% vs 5% at $t = 120$ s) is noted with $ArCr(CO)_3$/CCl_4 compared to $ArCr(CO)_3$. On the opposite, for all the investigated systems, the addition of TTMSS enhances the polymerization efficiency (Figure 6), albeit the polymerization rates are not very high. The polymerization rate remains quite low compared to classical type I photoinitiating systems. Concomitantly, a high Si−H consumption is observed during the polymerization (Figure 6) confirming the hydrogen abstraction process -14 (see above).

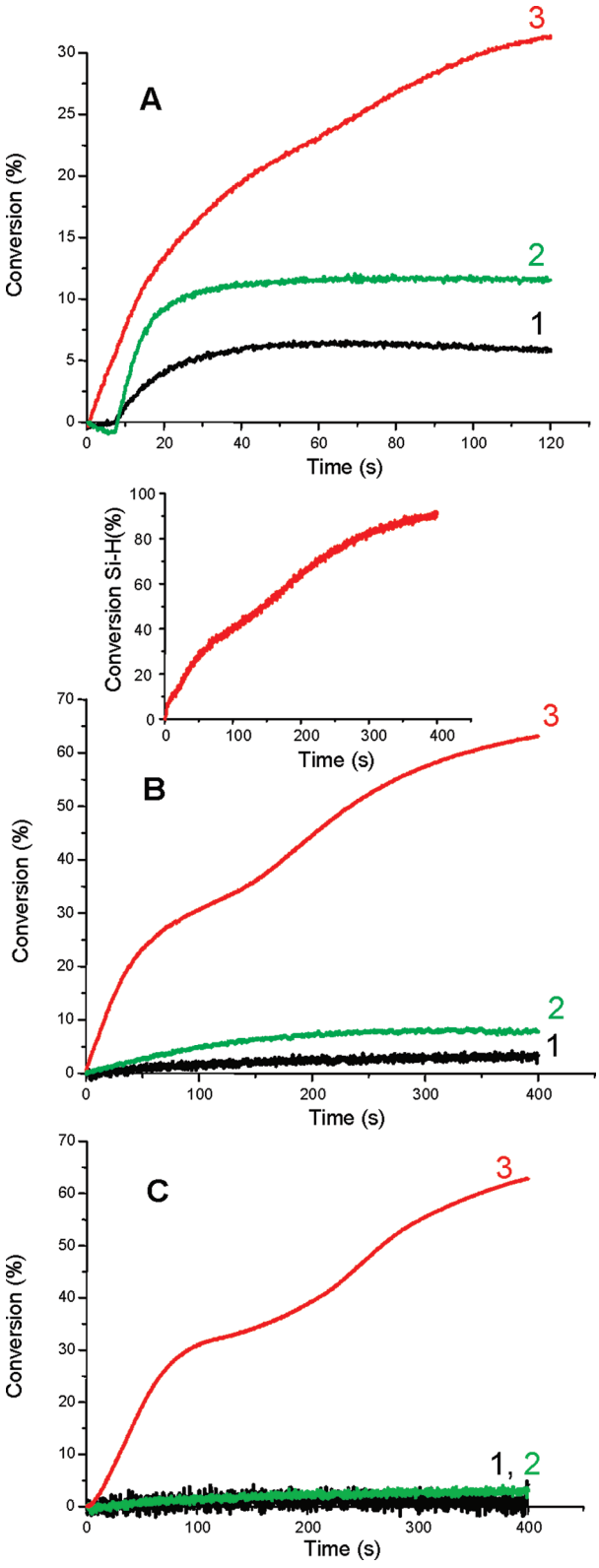

Figure 6. (A) Photopolymerization profiles of TMPTA under air upon a Xe−Hg lamp irradiation in the presence of (1) $ArCr(CO)_3$ (1% w/w), (2) $ArCr(CO)_3$/CCl_4 (1%/3% w/w), and (3) $ArCr(CO)_3$/TTMSS (1%/3% w/w). (B) Photopolymerization profiles of TMPTA under air upon a Xe−Hg lamp irradiation in the presence of (1) $Cp_2Mo_2(CO)_6$ (1% w/w), (2) $Cp_2Mo_2(CO)_6$/CCl_4 (1%/3% w/w), and (3) $Cp_2Mo_2(CO)_6$/TTMSS (1%/3% w/w). Inset: the Si−H conversion for point 3. (**C**) Photopolymerization profiles of TMPTA under air upon a Xe−Hg lamp irradiation in the presence of (1) $Cp_2Ru_2(CO)_4$ (1% w/w), (2) $Cp_2Ru_2(CO)_4$/CCl_4 (1%/3% w/w), and (3) $Cp_2Ru_2(CO)_4$/TTMSS (1%/3% w/w).

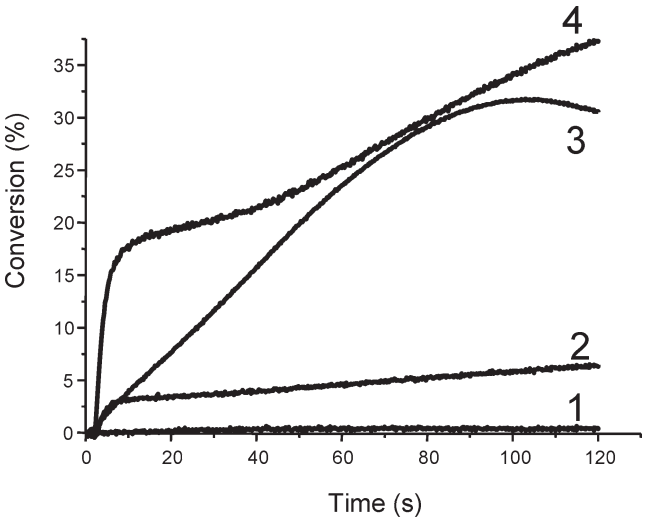

Figure 7. Photopolymerization profiles of TMPTA under air upon a Xe−Hg lamp irradiation (λ > 310 nm) in the presence of (1) $Cp_2Mo_2(CO)_6$ (1% w/w), (2) $Cp_2Mo_2(CO)_6$/CumOOH (1%/3% w/w), (3) $Cp_2Mo_2(CO)_6$/TTMSS (1%/3% w/w), and (4) $Cp_2Mo_2(CO)_6$/CumOOH/TTMSS (1%/3%/3% w/w).

The same holds true upon a diode laser irradiation at 405 nm despite a lower light intensity which increases the detrimental effect of O_2. These results unambiguously demonstrate that TTMSS is a better additive to **M-sub**s than the alkyl halides commonly proposed. The role of the hydroperoxide is also demonstrated under air (Figure 7). Addition of CumOOH to **M-Sub**/TTMSS clearly enhances the polymerization efficiency upon a Xe−Hg lamp irradiation thereby confirming that the decomposition of the hydroperoxides participates into the initiation mechanism.

5. FRPCP for Lamp and Laser Diode Visible Light Irradiations. When using **M-Sub**/Ph_2I^+ systems, only a very low conversion of EPOX can be reached after 400s (< 5%). Figures 8-9 show that the addition of TTMSS (3% w/w) to **M-Sub**/Ph_2I^+ dramatically improves the polymerization (except for $ArCr(CO)_3$) carried out under both diode laser and xenon lamp irradiations under air. An increase of [Ph_2I^+] leads to the increase of the consumption of the Si−H content (inset of Figure 9) and to the enhancement of the polymerization rates and final conversions (Figure 9). As for the FRP process, a high Si−H function consumption is observed during the polymerization (Figures 8 and 9) also demonstrating that a hydrogen abstraction process is involved in FRPCP. For $ArCr(CO)_3$, the lack of polymerization is ascribed to a detrimental quenching of $ArCr(CO)_2$ by EPOX ($\sim 2 \times 10^6$ M^{-1} s^{-1}). The vacant coordination site of this intermediate is likely occupied by a EPOX molecule. An oxygen lone pair of the epoxy function is probably involved as in the efficient CO addition reaction (rate constant: 3×10^7 M^{-1} s^{-1}[21]) shown in eq 17. This EPOX quenching is also probably competitive to the silyl radical formation since $ArCr(CO)_3$/TTMSS/Ph_2I^+ is no more an efficient system. Using the $Cp_2Mo_2(CO)_6$/TTMSS/Ph_2I^+ system, the cationic polymerization is very efficient upon the laser diode exposure at 405, 457, 473, and 532 nm (Figure 9 and the Supporting Information, Figure 2). In **M-Sub**/TTMSS/Ph_2I^+, the major pathway probably corresponds to the silyl radical formation and their oxidation by Ph_2I^+ leading to the initiating silylium cations. The decomposition of the hydroperoxides generated through 4 generates alkoxyl radicals which can be converted into silyl radicals by hydrogen abstraction 10. This latter process still increases the formation of $R_3Si^\bullet$. The radicals

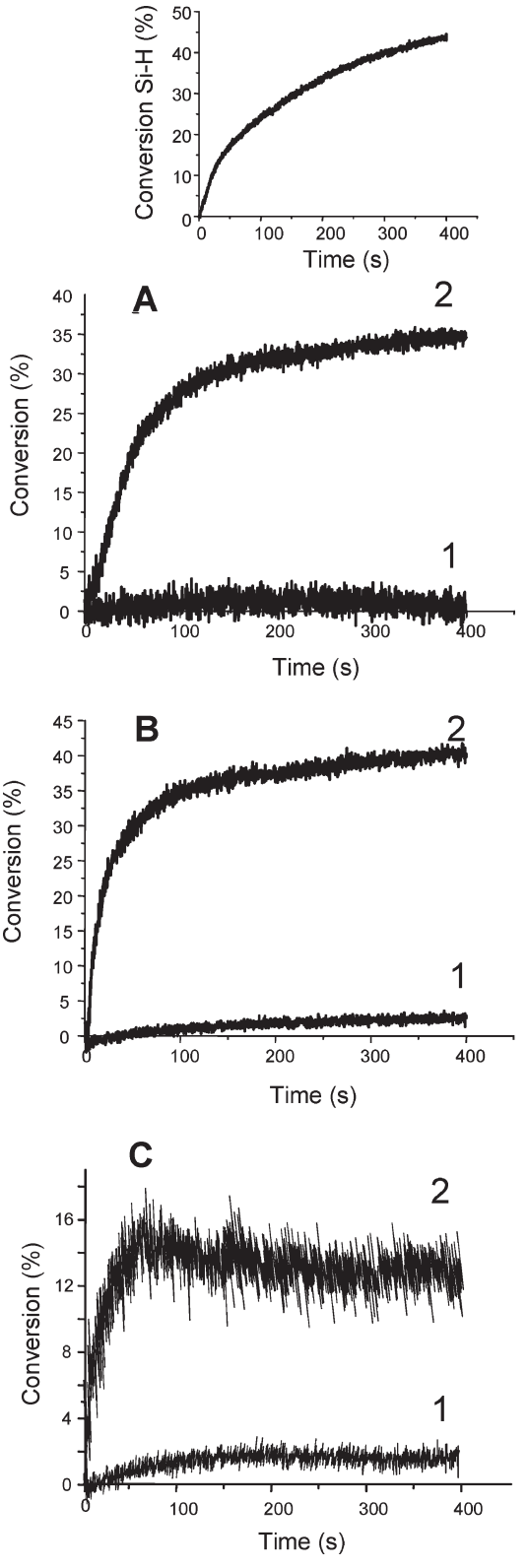

Figure 8. (**A**) Photopolymerization profiles of EPOX under air upon a xenon lamp irradiation (λ > 400 nm) in the presence of (1) $Fe_2(CO)_9$/Ph_2I^+ (1%/1% w/w); (2) $Fe_2(CO)_9$/TTMSS/Ph_2I^+ (1%/3%/1% w/w). Insert: the Si−H conversion for (2). (**B**) Photopolymerization profiles of EPOX under air upon a xenon lamp irradiation (λ > 400 nm) in the presence of (1) $Cp_2Mo_2(CO)_6$/Ph_2I^+ (1%/1% w/w); (2) $Cp_2Mo_2(CO)_6$/TTMSS/Ph_2I^+ (1%/3%/1% w/w). (**C**) Photopolymerization profiles of EPOX under air upon a xenon lamp irradiation (λ > 400 nm) in the presence of (1) $Cp_2Ru_2(CO)_4$/Ph_2I^+ (1%/1% w/w); (2) $Cp_2Ru_2(CO)_4$/TTMSS/Ph_2I^+ (1%/3%/1% w/w).

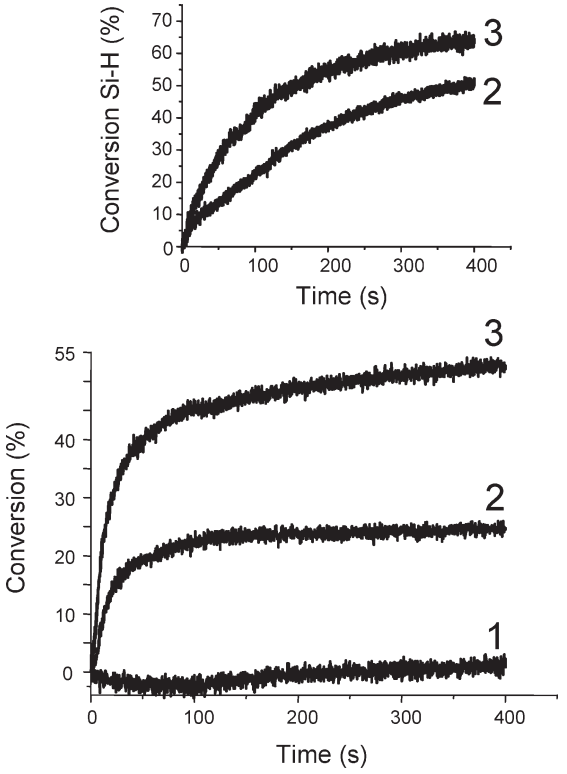

Figure 9. Photopolymerization profiles of EPOX under air upon a diode laser irradiation (532 nm) in the presence of (1) $Cp_2Mo_2(CO)_6$/Ph_2I^+ (1%/1% w/w), (2) $Cp_2Mo_2(CO)_6$/TTMSS/Ph_2I^+ (1%/3%/1% w/w), and (3) $Cp_2Mo_2(CO)_6$/TTMSS/Ph_2I^+ (1%/3%/2% w/w). Inset: the Si−H conversion for points 2 and 3.

generated in **M-Sub**/TTMSS/Ph_2I^+ are also able to initiate FRP (e.g., Figure 3 in the Supporting Infomation for **M-Sub** = $Cp_2Mo_2(CO)_6$).

$$ArCr(CO)_2 + CO \rightarrow ArCr(CO)_3 \qquad (17)$$

Conclusions

In the present paper, new metal-based **M-Sub** and silane-containing photoinitiating systems are proposed for FRPCP and FRP under polychromatic (lamp) and monochromatic light (filtered lamp, diode laser) exposure. In addition to the well-known ability of the silyl radical chemistry to overcome the oxygen inhibition, **the M-Sub**s allow here a decomposition of the hydroperoxides and an increase of the amount of initiating radicals. Since the light absorption properties of **M-Sub** as well as the reactivity of the generated metal-centered radicals can be tuned by an appropriate selection of the metals or the ligands, one should expect the development of such systems for applications under visible lights delivered by conventional sources or other lasers in the radiation curing and laser imaging areas. These systems are particularly attractive for FRPCP with excellent polymerization rates and final conversions.

Supporting Information Available: Figures showing FTIR spectra for TMPTA film in the presence of $ArCr(CO)_3$, photopolymerization profiles of EPOX under air upon a diode laser irradiation in the presence of $Cp_2Mo_2(CO)_6$/Ph_2I^+ or $Cp_2Mo_2(CO)_6$/TTMSS/Ph_2I^+, and photopolymerization profiles of TMPTA under air upon a Xe−Hg lamp irradiation ($\lambda > 310$ nm) in the presence of $Cp_2Mo_2(CO)_6$, $Cp_2Mo_2(CO)_6$/Ph_2I^+, and $Cp_2Mo_2(CO)_6$/Ph_2I^+/TTMSS. This material is available free of charge via the Internet at http://pubs.acs.org.

References and Notes

(1) (a) Pappas, S. P. *UV Curing: Science and Technologie II*; Technologie Marketing Corporation: 1985. (b) Crivello, J. V. *Photoinitiators for Free Radical, Cationic and Anionic Photopolymerization*, 2nd ed.; Bradley, G., Ed.; New York, 1998. (c) Dietliker, K. *A Compilation of Photoinitiators commercially available for UV today*; Sita Technology Ltd.: Edinburgh, London, 2002. (d) Neckers, D. C. *UV and EB at the Millenium*; Sita Technology: London, 1999. (e) Schwalm, R. *UV coatings: basics, recent developments and new applications*; Elsevier: Oxford, U.K., 2007. (f) Davidson, R. S. *Exploring the Science, Technology and Applications of UV and EB Curing*; SITA Technology Ltd.: London, 1999. (g) Krongauz, V.; Trifunac, A. *Photoresponsive Polymers*; Chapman and Hall: New-York, 1994. (h) Belfield, K.; Crivello, J. V. *Photoinitiated Polymerization*; ACS Symposium Series 847; American Chemical Society: Washington, DC, 2003.

(2) (a) Fouassier, J. P., Rabek, J. F., Eds. *Radiation Curing in Polymer Science and Technology*; Elsevier Science Publishers LTD: London, 1993. (b) Fouassier, J. P. *Photoinitiation, Photopolymerization and Photocuring: Fundamental and Applications*; Hanser Publishers: New-York, 1995; (c) *Photochemistry and UV Curing* Fouassier, J. P., Ed., Research Signpost: Trivandrum India, 2006. (d) *Basics of photopolymerization reactions*; Fouassier, J. P., Allonas, X., Eds.; Research Signpost: Trivandrum India, in press.

(3) (a) Ledwith, A. *Polymer* **1978**, *19*, 1217–1219. (b) Baumann, H.; Timpe, H. J. *Z. Chem.* **1984**, *24*, 18–19. (c) Yagci, Y.; Schnabel, W. *Makromol. Chem. Rapid Commun.* **1987**, *8*, 209–213. (d) Yagci, Y.; Ledwith, A. *J. Polym. Sci., Part A: Polym. Chem.* **1988**, *26*, 1911–1918. (e) Yagci, Y.; Kminek, I.; Schnabel, W. *Polymer* **1993**, *34*, 426–428. (f) Bi, Y.; Neckers, D. C. *Macromolecules* **1994**, *27*, 3683–3693. (g) Crivello, J. V.; Sangermano, M. *J. Polym. Sci. Part A: Chem* **2001**, *39*, 343–356. (h) Dursun, C.; Degirmenci, M.; Yagci, Y.; Jockusch, S.; Turro, N. J. *Polymer* **2003**, *44*, 7389–7396. (i) Durmaz, Y. Y.; Moszner, N.; Yagci, Y. *Macromolecules* **2008**, *41*, 6714–6718. (j) Crivello, J. V. *J. Polym. Sci., Part A: Polym. Chem.* **2009**, *47*, 866–875. (k) Crivello, J. V. *J. Macromol. Sci. Part A* **2009**, *46*, 474–483.

(4) Maillard, B.; Ingold, K. U.; Scaiano, J. C. *J. Am. Chem. Soc.* **1983**, *105*, 5095–5099.

(5) (a) Lalevée, J.; Blanchard, N.; El-Roz, M.; Graff, B.; Allonas, X.; Fouassier, J. P. *Macromolecules* **2008**, *41*, 4180–4186. (b) Lalevée, J.; El-Roz, M.; Allonas, X.; Fouassier, J. P. *J. Polym. Sci., Part A: Polym. Chem.* **2008**, *46*, 2008–2014. (c) Tehfe, M. A.; Lalevée, J.; Allonas, X.; Fouassier, J. P. *Macromolecules* **2009**, *42*, 8669–8674.

(6) (a) El-Roz, M.; Lalevée, J.; Allonas, X.; Fouassier, J. P. *Macromolecules* **2009**, *42*, 8725–8732. (b) Lalevée, J.; Allonas, X.; Fouassier, J. P. *Chem. Phys. Lett.* **2009**, *469*, 298–303.

(7) (a) Lalevée, J.; Dirani, A.; El-Roz, M.; Allonas, X.; Fouassier, J. P. *J. Polym. Sci., Part A: Polym. Chem.* **2008**, *46*, 3042–3047. (b) Tehfe, M.-A.; Lalevée, J.; Gigmes, D.; Fouassier, J.-P. *Macromolecules* **2010**, *43*, 1364–1370. (c) Souane, R.; Tehfe, M. A.; Lalevée, J.; Gigmes, D.; Fouassier, J. P., *Macromol. Chem. Phys.* **2010**, *211*, 1441−1445.

(8) Lalevée, J.; Dirani, A.; El-Roz, M.; Allonas, X.; Fouassier, J. P. *Macromolecules* **2008**, *41*, 2003–2010.

(9) Zhu, Z.; Espenson, J. H. *Organometallics* **1994**, *13*, 1893–1898.

(10) Cunningham Jr, A. F.; Desobry, V. In *Radiation Curing in Polymer Science and Technology*; Fouassier, J. P., Rabek, J. F., Eds.; Elsevier Science Publishers Ltd.: London, 1993, Vol. *2*, 323−374.

(11) (a) Bamford, C. H. *Pure Appl. Chem.* **1973**, *34*, 173–191. (b) Bamford, C. H.; Mullik, S. U. *J. Chem. Soc., Faraday Trans. 1* **1977**, *73*, 1260–1270. (c) Bamford, C. H.; Al-Lamee, K. G.; Konstantinov, C. J. *J. Chem. Soc., Faraday Trans. 1* **1977**, *73*, 1406–1419. (d) Bamford, C. H.; Mullik, S. U. *J. Chem. Soc., Faraday Trans. 1* **1976**, *72*, 368–375. (e) Bamford, C. H.; Mullik, S. U. *J. Chem. Soc., Faraday Trans. 1* **1979**, *75*, 2562–2575. (f) Bamford, C. H.; Al-Lamee, K. G. *J. Chem. Soc., Faraday Trans. 1* **1984**, *80*, 2175–2186. (g) Yagci, Y.; Hepuzer, Y. *Macromolecules* **1999**, *32*, 6367–6370. (h) Tehfe, M. A.; Lalevée, J.; Gigmes, D.; Fouassier, J. P. *J. Polym. Sci., Part A: Polym. Chem.* **2010**, *48*, 1830–1837.

(12) Kunding, E. P.; Xu, L. H.; Kondratenko, M.; Cunningham, A. F., Jr; Kuntz, M. *Eur. J. Inorg. Chem.* **2007**, *18*, 2934–2943.

(13) Tordo, P. *Spin-trapping: recent developments and applications*; Atherton, N. M., Davies, M. J., Gilbert, B. C., Eds., Electron Spin Resonance 16; The Royal Society Of Chemistry: Cambridge, U.K., 1998.

(14) (a) Criqui, A.; Lalevée, J.; Allonas, X.; Fouassier, J. P. *Macromol. Chem. Phys.* **2008**, *209*, 2223–2231. (b) Guo, Q.; Qian, S. Y.; Mason, R. P. *J. Am. Soc. Mass Spectrom.* **2003**, *14*, 862–871.

(15) Lalevée, J.; Allonas, X.; Fouassier, J. P. *J. Am. Chem. Soc.* **2002**, *124*, 9613–9621.

(16) (a) Gasanov, R. G.; Dotdaev, S. K. *Russ. Chem. Bull.* **1986**, *35*, 1801–1805. (b) Gasanov, R. G.; Freidlina, R. K. *Russ. Chem. Bull.* **1981**, *30*, 980–984.
(17) Chatgilialoglu, C. *Organosilanes in Radical Chemistry*; Wiley: Chichester, U.K., 2004.
(18) Lalevée, J.; Allonas, X.; Fouassier, J. P. *J. Org. Chem.* **2007**, *72*, 6434–6436.
(19) (a) Hudson, A.; Lappert, M. F.; Lednor, P. W.; Nicholson, B. K. *J. Chem. Soc., Chem. Comm.* **1974**, 966–967. (b) Hudson, A.; Lappert, M. F.; Nicholson, B. K. *J. Chem. Soc., Dalton Trans.* **1977**, 551–554. (c) Macyk, W.; Herdegen, A.; Karocki, A.; Stochel, G.; Stasicka, Z.; Sostero, S.; Traverso, O. *J. Photochem. Photobiol. A: Chem.* **1997**, *103*, 221–226. (d) Balla, J.; Bakac, A.; Espenson, J. H. *Organometallics* **1994**, *13*, 1073–1074. (e) Bitterwolf, T. E. *J. Organomet. Chem.* **2004**, *689*, 3939–3952.
(20) (a) Espenson, J. H. *J. Mol. Liq.* **1995**, *65/66*, 205–212. (b) Scott, S. L.; Espenson, J. H.; Zhu, Z. *J. Am. Chem. Soc.* **1993**, *115*, 1789–1797.
(21) Creaven, B. S.; George, M. W.; Ginzburg, A. G.; Hughes, C.; Kelly, J. M.; Long, C.; McGrath, I. M.; Pryce, M. T. *Organometallics* **1993**, *12*, 3127–3131.
(22) Fletcher, S. C.; Poliakoff, M.; Turner, J. J. *Inorg. Chem.* **1986**, *25*, 3597–3604.
(23) (a) Gaussian 03, Revision B.2, Frisch, M. J.; Trucks, G. W.; Schlegel, H. B.; Scuseria, G. E.; Robb, M. A.; Cheeseman, J. R.; Zakrzewski, V. G.; Montgomery, J. A., Jr.; Stratmann, R. E.; Burant, J. C.; Dapprich, S.; Millam, J. M.; Daniels, A. D.; Kudin, K. N.; Strain, M. C.; Farkas, O.; Tomasi, J.; Barone, V.; Cossi, M.; Cammi, R.; Mennucci, B.; Pomelli, C.; Adamo, C.; Clifford, S.; Ochterski, J.; Petersson, G. A.; Ayala, P. Y.; Cui, Q.; Morokuma, K.; Salvador, P.; Dannenberg, J. J.; Malick, D. K.; Rabuck, A. D.; Raghavachari, K.; Foresman, J. B.; Cioslowski, J.; Ortiz, J. V.; Baboul, A. G.; Stefanov, B. B.; Liu, G.; Liashenko, A.; Piskorz, P.; Komaromi, I.; Gomperts, R.; Martin, R. L.; Fox, D. J.; Keith, T.; M. A. Al-Laham, Peng, C. Y.; Nanayakkara, A.; Challacombe, M.; Gill, P. M. W.; Johnson, B.; Chen, W.; Wong, M. W.; Andres, J. L.; Gonzalez, C.; M. Head-Gordon, Replogle, E. S.; , Pople, J. A., Gaussian, Inc.: Pittsburgh PA, 2003. (b) Foresman, J. B.; Frisch, A. *Exploring Chemistry with Electronic Structure Methods*, 2nd ed.; Gaussian. Inc.: Pittsburgh, PA, 1996.